

General Disclaimer

One or more of the Following Statements may affect this Document

- This document has been reproduced from the best copy furnished by the organizational source. It is being released in the interest of making available as much information as possible.
- This document may contain data, which exceeds the sheet parameters. It was furnished in this condition by the organizational source and is the best copy available.
- This document may contain tone-on-tone or color graphs, charts and/or pictures, which have been reproduced in black and white.
- This document is paginated as submitted by the original source.
- Portions of this document are not fully legible due to the historical nature of some of the material. However, it is the best reproduction available from the original submission.

(NASA-TM-X-74037) A NEW CAPABILITY FOR
PREDICTING HELICOPTER ROTOR AND PROPELLER
NOISE INCLUDING THE EFFECT OF FORWARD MOTION
(NASA) 25 p HC A02/MF A01 CSCL 20A

N77-27876

G3/71 Unclass
36818

NASA TECHNICAL MEMORANDUM

NASA TM X-74037

NASA TM X-74037

A NEW CAPABILITY FOR PREDICTING HELICOPTER ROTOR AND
PROPELLER NOISE INCLUDING THE EFFECT OF FORWARD
MOTION

By

F. Farassat
George Washington University

and

T. J. Brown
U. S. Army Air Mobility Research and Development Lab

June 1977

This informal documentation medium is used to provide accelerated or special release of technical information to selected users. The contents may not meet NASA formal editing and publication standards, may be revised, or may be incorporated in another publication.

**NATIONAL AERONAUTICS AND SPACE ADMINISTRATION
LANGLEY RESEARCH CENTER, HAMPTON, VIRGINIA 23665**



A NEW CAPABILITY FOR PREDICTING HELICOPTER ROTOR AND
PROPELLER NOISE INCLUDING THE EFFECT OF FORWARD
MOTION

By F. Farassat* and T. J. Brown

SUMMARY

This paper discusses the governing equation and computing technique for the prediction of helicopter rotor and propeller noise. The method which gives both the acoustic pressure time history and spectrum of the noise includes the thickness and the loading noise. It has been effectively adapted to computers resulting in a new capability in noise prediction by removing many of the restrictions and limitations of previous theories. The capability results from the fact that the theory is developed entirely in the time domain in contrast to most previous works which were developed in frequency domain. The formulation and the technique used is not limited to compact sources, steady level flight or to the far-field. In addition, the inputs to the computer program are normally available or are amenable to experimental measurements. This program can be used to study rotor and propeller noise with the aim of minimizing the radiated noise to reduce annoyance to the public. Several examples demonstrating the features and capability of the computer program are presented.

INTRODUCTION

The problem of noise radiation from propellers and helicopter rotors has gained prominence due to its annoyance to the public. Although a helicopter rotor is one of the several noise generating sources of helicopters, it is most important in the external regions of the present machines. Large propellers are currently under study for propulsion of large airliners with cruise speed of about 850 km/h. The good fuel efficiency of such propulsion systems is the main reason for their consideration. Clearly, the reliable prediction of the noise of propellers and rotors in the design stage of the aircraft is an important step in controlling the level of the noise intensity.

There has been a steady advance in the last decade in the prediction of the noise of rotating blades (ref. 1). There are still disagreements between the theoretical and experimental results. The available theories suffer from a combination of the following restrictions:

*The first author acknowledges support from U. S. Army Research Office.

- a. Compactness of the acoustic sources
- b. Hovering rotor or static propeller
- c. Observer in the far field
- d. Limited airfoil shapes
- e. Limited surface pressure distribution models
- f. Singularities in the solution for high blade tip speeds
- g. Neglect of the thickness noise
- h. Blades with rectangular planforms

It is believed that the removal of these restrictions and the inclusion of the nonlinear propagation effects should result in reliable prediction of the rotating blade noise.

Traditionally, rotor noise has been divided into several categories such as rotational, vortex and thickness noise. Propeller noise theories consider steady thrust and torque forces. However, the acoustic sources are almost always assumed compact. Theoretically, the acoustic sources may be grouped into two broad classes - those depending on the local pressure and viscous stress distribution on the blades and those due to the normal velocity distribution on the blades. For example, rotational noise belongs to the first class and thickness noise to the second. A theory which incorporates the effects of surface pressure and normal velocity distribution on a moving body is developed in reference 2. The formulation is then specialized for propellers and helicopter rotors. In this work a study of compactness assumption of sources on moving bodies has revealed that in the case of helicopter rotors and propellers, the sources on the blades cannot be considered compact for the observer position in a large region of space around the rotor. If the compactness restriction is removed, then one would like to remove the restrictions of limited airfoil, limited airfoil shapes and surface pressure distribution models to improve the prediction technique.

The present paper discusses the governing equation and the computing technique together with a computer program developed by the authors at NASA Langley Research Center based on the results of reference 2. The purpose of developing this program has been to remove the restrictions mentioned above and thus improve the prediction of the rotor and propeller noise. The acoustic computation is performed in the time domain and the resulting pressure signature is then Fourier analyzed to get the acoustic pressure spectrum.

The new program can only handle deterministic pressure distribution on the blades. It is known that the random unsteady pressure fluctuations on the blades have significant effect on the noise field of rotating blades when the sources can be considered compact. At relatively high tip speeds, particularly in forward flight, the unsteady pressure fluctuations are small compared to the steady component on propeller blades (ref. 3). At high advancing tip speeds, it appears that the random fluctuating pressure of the rotor blades has small effect on the acoustic field in the region of space where the acoustic sources should be considered noncompact. It must be mentioned that the compactness of sources is not a property of the sources per se but depends on the observer position as well as the motion and extent of the sources.

Examples are presented in this paper to demonstrate the broad range of problems which may be handled by this new program. These examples are selected mainly with regard to the restrictions discussed earlier which are removed by the new formulation.

SYMBOLS

c	speed of sound (m/sec)
C_1 to C_5	constants describing airfoil shape
CH	blade chord as function of η_2 (m)
E	dimensionless variable η_1'/CH
E_r	dimensionless variable η_2/R
$f(\vec{y}, \tau)=0$	equation describing the surface of each blade
$g=\tau-t+r/c=0$	the equation of a collapsing sphere for a fixed \vec{x} and t
I_1 to I_5	integrals given by equations (3) to (7)
LE	equation of leading edge of the blade as a function of η_2
p	surface pressure of the blade (N/m^2)
p'	acoustic pressure (N/m^2)
p_L	pressure on the lower surface of airfoil (N/m^2)
p_U	pressure on the upper surface of the airfoil (N/m^2)
p_S	$(p_L + p_U)/2$ (N/m^2)
r	$ \vec{x} - \vec{y} $
R	rotor radius (m)
t	observer time (sec)
T	blade thickness ratio as a function of η_2 (given as fraction of 1), y_{max}/CH
TE	equation of trailing edge of the blade as a function of η_2

y	airfoil coordinate given usually as $y=T \text{ CH}(C_1 E^{\frac{1}{2}} + C_2 E + C_3 E^2 + C_4 E^3 + C_5 E^4)$ (m)
\vec{y}	source position in a frame fixed to undisturbed medium
\vec{x}	observer position in a frame fixed to undisturbed medium
α	blade angle of attack as a function of η_2
Γ	the curve of intersection of $g=0$ and $f=0$ or $g=0$ and the mean plane of each blade
Δp	pressure differential $p_L - p_U$ (local lift/unit area) (N/m^2)
η_1	coordinate axis fixed to each blade in chordwise direction increasing from leading edge to trailing edge
η_1'	same as η_1 -axis but with the origin at the leading edge
η_2	coordinate axis fixed to each blade in spanwise direction with origin at the rotor center increasing towards the blade tip
θ	the angle between radiation direction $\vec{x} - \vec{y}$ and the normal to blade surface
ρ_0	density of the undisturbed medium
τ	source time (sec)
τ_1, τ_2	the source times when the sphere $g=0$ enters and leaves the blade system, respectively (sec)

THE ACOUSTIC FORMULATION

The formulation derived in reference 2 is briefly discussed here. Consider a moving body whose surface is described by $f(\vec{y}, \tau)=0$ where τ is the source time. Let v_n be the local normal velocity of the surface, the acoustic pressure $p'(\vec{x}, t)$ is given by

$$\begin{aligned}
4\pi p'(\vec{x}, t) = & \frac{\partial}{\partial t} \int_{\tau_1}^{\tau_2} \int_{\Gamma} \frac{\rho_0 c v_n + p \cos \theta}{r \sin \theta} d\Gamma d\tau \\
& + c \int_{\tau_1}^{\tau_2} \int_{\Gamma} \frac{p \cot \theta}{r^2} d\Gamma d\tau
\end{aligned} \tag{1}$$

The computer program is written in such way that the contributions of the upper and lower surfaces of the blades to the acoustic pressure p' are summed separately as follows. Let the subscripts U and L stand for upper and lower surfaces of the blades. If p_S and Δp are defined by the following relations

$$p_S = \frac{1}{2} (p_L + p_U)$$

$$\Delta p = p_L - p_U, \text{ (local lift/unit area)}$$

then, we get

$$p_U = p_S - \frac{\Delta p}{2}$$

$$p_L = p_S + \frac{\Delta p}{2}$$

Equation (1) is then written as

$$p'(\vec{x}, t) = \frac{\partial}{\partial t} [I_1 + I_2 + I_3] + I_4 + I_5 \tag{2}$$

The expressions for I_1 to I_5 are

$$I_1 = \frac{\rho_0 c}{4\pi} \int_{\tau_1}^{\tau_2} \int_{\Gamma} \frac{1}{r} [(v_n \operatorname{cosec} \theta)_U + (v_n \operatorname{cosec} \theta)_L] d\Gamma d\tau \tag{3}$$

$$I_2 = -\frac{1}{8\pi} \int_{\tau_1}^{\tau_2} \int_{\Gamma} \frac{\Delta p}{r} [\cot \theta_U - \cot \theta_L] d\Gamma d\tau \tag{4}$$

$$I_3 = \frac{1}{4\pi} \int_{\tau_1}^{\tau_2} \int_{\Gamma} \frac{p_S}{r} [\cot \theta_U + \cot \theta_L] d\Gamma d\tau \tag{5}$$

$$I_4 = -\frac{1}{8\pi} \int_{\tau_1}^{\tau_2} \int_{\Gamma} \frac{\Delta p}{r^2} [\cot \theta_U - \cot \theta_L] d\Gamma d\tau \quad (6)$$

$$I_5 = \frac{1}{4\pi} \int_{\tau_1}^{\tau_2} \int_{\Gamma} \frac{p_S}{r^2} [\cot \theta_U + \cot \theta_L] d\Gamma d\tau \quad (7)$$

The curve Γ is now the intersection of the sphere $g = \tau - t + r/c = 0$ and the mean surface of the blades. The method of computation of the above integrals are discussed in the next section.

The integral I_1 describes the thickness noise. The sum of I_2 to I_5 will be referred to as surface pressure or loading noise. Aerodynamic calculations generally involve the evaluation of Δp . The pressure p_S is usually not available. The contribution of the integrals involving p_S to the overall noise $p'(\vec{x}, t)$ appears to be small compared to the dominating term in Eq. (2).

COMPUTATIONAL METHOD

Equations (3) to (7) are evaluated on a computer using a double numerical integration followed by numerical smoothing and differentiation where required. Each of the five integrals are integrated separately. The first three are subsequently differentiated and the resulting five pressure contributions are added to obtain the pressure signature and spectrum.

At source $\tau = \tau_i$ a sphere is constructed with its center at the observer location. Its radius r_i is selected such that its circle of intersection, C' , with the plane of the rotor is tangent to the rotor disk. From this initial geometry the initial observer time, t_i , is calculated from $t_i = \tau_i + r_i/c$ where c is the speed of sound in the medium. The sphere is allowed to collapse by an amount $c\Delta\tau$, where τ is the emission or source time. During this period, the helicopter rotor is allowed to translate and rotate. The resulting arc of intersection between the rotor disk and the new C' is swept point by point in a counterclockwise direction until an intersection with a blade surface is detected or until the arc passes out of the rotor disk. When a blade is encountered, the integrands of equations (3) to (7) are evaluated and subsequently the line integrals are accumulated point by point using a trapezoidal scheme.

The collapsing process of the sphere $g = 0$ is repeated, each time yielding a value for the line integrals which are accumulated for the source time integration using Simpson rule. This process is continued until it is detected that the collapsing sphere has passed out of the rotor disk. The integration

is thus concluded for the observer time t_i and the resulting integrals are saved for further processing. Successive points are obtained in like manner.

To facilitate numerical smoothing and differentiation with respect to the observer time t , it is required that the t_i 's be equally spaced. Since the relation between the observer time t and the source time τ is in general nonlinear, an iteration technique is used to obtain the initial radius r_i and the corresponding source time τ_i where the sphere $g = 0$ begins to collapse. The smoothing and numerical differentiation which is used are presented in reference 4. It is based on the theory of finite Fourier series using factors which modify harmonic levels to improve convergence characteristics and to reduce Gibbs phenomenon. As a byproduct of this, the pressure spectrum of the acoustic signature is obtained quite easily using intermediate results of the smoothing and differentiation process.

The observer may be assumed fixed in the moving frame attached to the vehicle. In this case two-point time differentiation is used while the observer position is frozen with respect to the undisturbed medium. For a new observer time, the observer is moved to its original position in the moving frame and the process is repeated.

SOME APPLICATIONS OF THE COMPUTER PROGRAM

The examples in this section are selected with realistic data to demonstrate the features and capability of the computer program. In all the calculations, the source distribution is noncompact. In each example, the assumptions and the needed data used in computation are given. In two cases, experimental measurements are also available and are presented together with theoretical results.

EXAMPLE 1 - Helicopter noise

The special features of this example are:

- i) helicopter in flight,
- ii) triangular blade tips and blades with twist,
- iii) realistic rotor attitude - tip path plane does not contain the forward velocity vector.

Because of the high advancing blade tip speed and the observer location, only thickness noise is believed to be dominant and therefore is calculated. The pressure distribution on the blades was not available.

INPUT DATA:

Number of blades = 2

R = 7.62 m

RPM = 300

$$CH(\eta_2) = \begin{cases} 0.838 \text{ m} & \eta_2 \leq 7.322 \text{ m} \\ -2.246 \eta_2 + 17.283 & 7.322 < \eta_2 \leq 7.62 \text{ m} \end{cases}$$

$$T(\eta_2) = \begin{cases} 0.1 & \eta_2 \leq 7.322 \text{ m} \\ -0.1678 \eta_2 + 1.3286 & 7.322 < \eta_2 \leq 7.62 \text{ m} \end{cases}$$

$$LE(\eta_2) = \begin{cases} -0.335 \text{ m} & \eta_2 \leq 7.322 \text{ m} \\ 2.246 \eta_2 - 16.780 \text{ m} & 7.322 < \eta_2 \leq 7.62 \text{ m} \end{cases}$$

$$TE(\eta_2) = 0.503 \text{ m}$$

$$\alpha(\eta_2) = -8.0 + 1.05 \eta_2 \quad \text{degrees}$$

$$y(\eta_1', \eta_2) = T(\eta_2) CH(\eta_2) (3.3333 E - 6.5079 E^2 + 3.1746 E^3) \text{ m}$$

$$c = 340. \text{ m/sec}$$

Helicopter speed = 259.3 km/h (140 knts), level flight

Helicopter altitude = 152.5 m (500 ft)

Observer position (at emission time) = 439.6 m (1441.3 ft) directly ahead of helicopter at ground level (Fig. 1).

Rotor angle of attack = 6.5 degrees

Figure (1) shows the calculated and experimental acoustic pressure signatures. The experimental pressure signature includes the tail rotor noise. The helicopter speed and altitude used in this example are those recorded from the aircraft instruments. The emission distance is, however, an estimate obtained from approximate overhead position of the helicopter. The test helicopter has blades with Wortmann FX69-H-098 airfoil section which has a small leading edge radius. The airfoil section used in calculations is biconvex cubic shape approximating the actual airfoil section. Based on manufacturer supplied noise

data, the calculated sound pressure level is good. As seen from Figure 1, the agreement between the shape of the theoretical and measured signature is also good.

EXAMPLE 2 - Propeller noise

The special features of this example are:

- i) blades with twist and variable thickness
- ii) observer in motion with the aircraft

The power absorbed by the propeller was available in this case and the pressure distribution Δp was used in the calculation. This distribution is thought to be realistic. To simplify the calculation of this distribution, the blade planform is assumed rectangular. The actual blades on the test aircraft had a slight taper. The blade form curves are presented in Fig. 2. The thickness ratio and blade twist are approximated using the curves in this figure.

INPUT DATA:

Number of blades = 3

$R = 1.30 \text{ m}$

RPM = 2145

CH = 0.156 m (uniform, taken as chord at .85 R)

$T(\eta_2) = 0.069 + 3.2244 \exp(-8.615 \eta_2)$

$\alpha(\eta_2) = 3.61 + 78.037 \exp(-2.685 \eta_2) \text{ degrees}$

$y(\eta_1', \eta_2) = CH T(\eta_2) (3.3333 E - 6.5079 E^2 + 3.1746 E^3)$

$c = 345 \text{ m/sec}$

Aircraft speed = 144.5 km/h (78 KTS)

Observer position (in disk plane) = 7.28 m from propeller center moving with aircraft.

$\Delta p(\eta_1', \eta_2) = 2.507 \times 10^5 E^{.125} (1-E)^{.5} E_r^{2.833} (1-E_r)^{.5} \text{ N/m}^2$

Figure (3) shows the calculated and measured acoustic pressure signature and spectrum. The agreement both in time domain and frequency domain is very good. Note that although steady source distribution is used, the high harmonics of the acoustic pressure spectrum are calculated with reasonable accuracy. For propellers in motion, the blade geometry and steady blade surface pressure distribution are believed to be sufficient for prediction of the generated noise.

EXAMPLE 3 - Rotating Blades

The special features of this example are:

- i) supersonic tip speed
- ii) The blade surface pressure distributions Δp and p_s are included in noise calculation

To study the contribution of the terms involving p_s to the acoustic pressure, this example was devised. In general, p_s is not available and is not calculated usually. This is because p_s does not contribute to the lift, thrust, or the torque on the engine. Linearized aerodynamic theory is used to calculate Δp and p_s assuming that at each radial position, the flow around the blade is two dimensional. The flow around the entire blade is supersonic. A uniform downwash of 40 m/sec with tip Mach number of 1.375 are assumed. The blade Mach number at the inner radius is 1.10. The blade disk is assumed to be static.

INPUT DATA:

Number of blades = 2

$R = 5.0$ m

Inner blade radius = 4.0 m (Blade length = 1m)

RPM = 906.0

$CH(\eta_2) = 0.4$ m

$T(\eta_2) = 0.05$

$$\alpha(\eta_2) = \frac{6.643}{M_L} + \frac{0.768\sqrt{M_L^2 - 1}}{M_L^2} \text{ degrees,}$$

$M_L = \eta_2 \Omega / c$ (Local Mach Number),

Ω = angular velocity of the blades

$$y(\eta'_1, \eta_2) = \begin{cases} 0.05\eta'_1 \text{ m} & 0 \leq \eta'_1 \leq 0.2 \text{ m} \\ 0.02(1 - 2.5\eta'_1) \text{ m} & 0.2 < \eta'_1 \leq 0.4 \text{ m (diamond section)} \end{cases}$$

Observer position (in plane) = 15 m from disk center

Observer position (out of plane) = 30° above disk plane and 15 m from disk center.

$$\Delta p(\eta_1', \eta_2) = 3840.0 \text{ N/m}^2$$

$$p_S(\eta_1', \eta_2) = \begin{cases} 7.159 \times 10^3 M_L^2 / \sqrt{M_L^2 - 1} \text{ N/m}^2 & 0 < \eta_1' < 0.2 \text{ m} \\ -7.159 \times 10^3 M_L^2 / \sqrt{M_L^2 - 1} \text{ N/m}^2 & 0.2 < \eta_1' < 0.4 \text{ m} \end{cases}$$

Figure (4) presents the separate contributions of each term in Eq. (2) to $p'(\vec{x}, t)$ together with $p'(\vec{x}', t)$ both in time and frequency domains. For both observer positions, the acoustic pressure $p'(\vec{x}, t)$ is dominated by the thickness noise. The shapes of the acoustic pressure signature and spectrum for the observer in the disk plane are substantially different from those for the observer above the plane. This signifies a complex wave structure rotating in or near the plane containing the blade disk (not necessarily in the near field only).

In the plane of the disk, the contribution of the term involving p_S is larger than that due to Δp . These contributions are of the same phase. Above the plane this trend reverses although the contribution of p_S term is still relatively large. Since the thickness noise is significantly higher than other contributions, the inclusion of terms I_2 to I_5 produces small changes in the acoustic pressure signature and spectrum. However, for high tip speeds, if the effect of Δp is included in the calculations, one should also include the effect of p_S . Some calculations at subsonic tip speeds have shown that the contributions of the terms involving p_S is smaller than the other terms. However, this requires further study.

EXAMPLE 4 - (Helicopter rotor)

The special feature of this example is blades with swept back tips. Only thickness noise is calculated. This example is worked out to show the favorable effect of nonrectangular blade planform.

INPUT DATA

Number of blades = 2

R = 5.0 m

RPM = 527.1

CH(η_2) = 0.4 m (see Fig. 5)

T(η_2) = 0.08

$$LE(\eta_2) = \begin{cases} -0.2 \text{ m} & \eta_2 < 4.25 \text{ m} \\ -3.019 + 0.6633 \eta_2 \text{ m} & 4.25 < \eta_2 \leq 5 \text{ m} \end{cases}$$

$$TE(\eta_2) = \begin{cases} 0.2 \text{ m} & \eta_2 < 4.25 \text{ m} \\ -2.619 + 0.6633 \eta_2 \text{ m} & 4.25 < \eta_2 < 5 \text{ m} \end{cases}$$

$$\alpha(\eta_2) = 0$$

$$y(\eta_1, \eta_2) = 0.064 (E - E^2) \text{ biconvex parabolic}$$

$$c = 345 \text{ m/sec}$$

Helicopter speed = 248.4 km/h (134.1 kts) level flight

Observer position (in rotor plane) = 50. m from rotor center at the start of emission

Figure 5 presents the calculated acoustic pressure signature and spectrum (thickness noise). For comparison the corresponding results for a rotor with rectangular blades (CH = 0.4 m) are presented. For the rotor with rectangular blades, all the input data (except, of course, for $TE(\eta_2)$ and $LE(\eta_2)$) are identical to those given above. It is seen that the sweep at the blade tip has considerable influence in the shape and the peak values of the acoustic pressure signature. As compared to that of rectangular blades the acoustic pressure spectrum shows reduction in the case of swept back blades up to the 30th harmonic. The maximum reduction is about 6 dB at about 15th harmonic. This example demonstrates that the planform variation should be considered a promising method of controlling the noise of helicopter rotors and propellers.

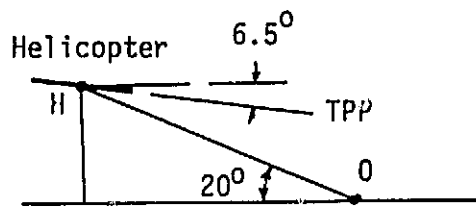
CONCLUSIONS

This paper presents a new formulation and a discussion of the method of computation of helicopter rotor and propeller noise. Only deterministic time dependent blade surface pressure may be used in the computer program that has been developed based on the new formulation. There are many situations where the unsteady random pressure fluctuations do not contribute substantially to the acoustic pressure. The most common of these is in the case of rotating blades at high tip speeds. The examples in this paper demonstrate the range of applicability of the computer program. By removing the restrictions and limitations of previous theories, it provides a capability which will improve the prediction and reduction of rotor and propeller noise.

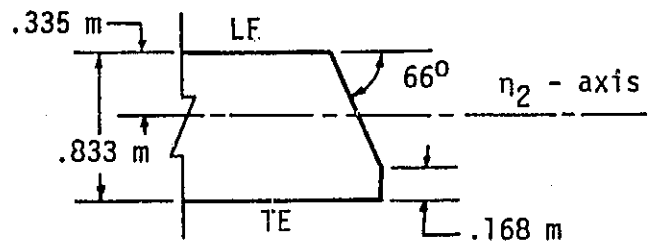
Random unsteady pressure fluctuations are important in regions where the acoustic sources are compact. They appear to be also important for static propellers and hovering rotors even in the regions where the acoustic sources are noncompact [ref. 3]. This is because of the injection of atmospheric turbulent eddies. In this case, a combined noncompact source calculation for thickness and steady loading noise and compact source calculation for unsteady loading noise appears to be the best choice.

REFERENCES

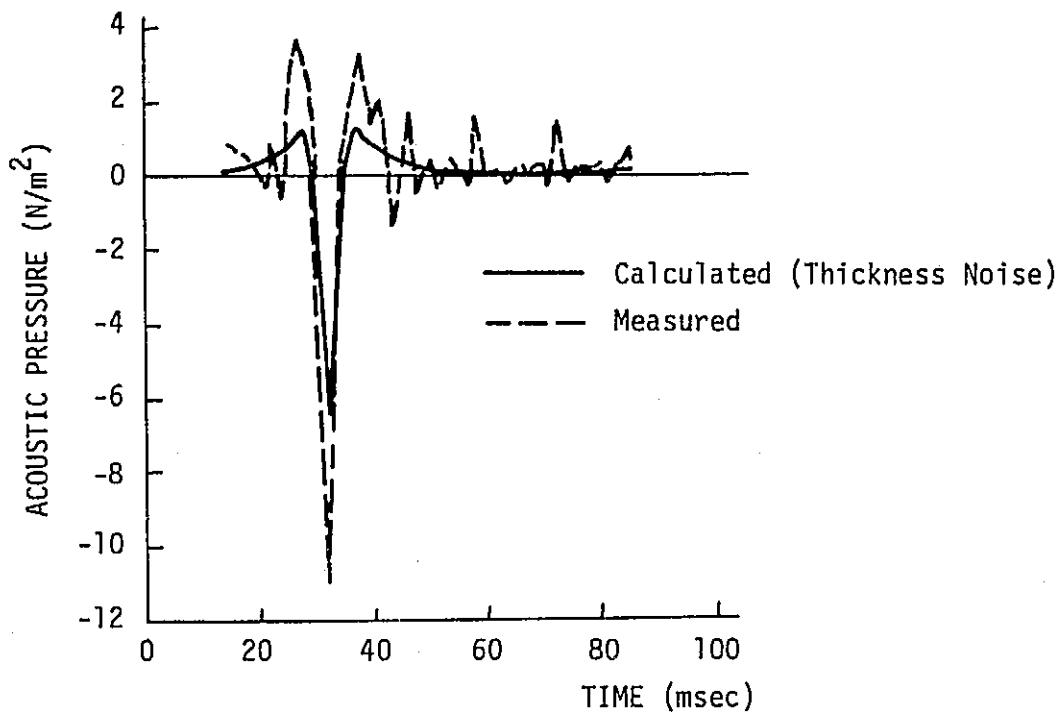
1. B. Magliozzi, F. B. Metzger, W. Bausch, R. J. King: A Comprehensive Review Of Helicopter Noise Literature, Rep. No. FAA-RD-75-79, U.S. Department of Transportation, June 1975.
2. F. Farassat: Theory Of Noise Generation From Moving Bodies With An Application To Helicopter Rotors, NASA Technical Report TR R-451, December 1975.
3. R. J. Pegg, B. Magliozzi, F. Farassat: Some Measured And Calculated Effects Of Forward Velocity On Propeller Noise, ASME Paper No. 77-GT-70, Presented to the Gas Turbine Division of ASME at the Gas Turbine Conference and Product Show, Philadelphia, PA, March 27-31, 1977.
4. C. Lanczos: Applied Analysis, Prentice Hall, Inc., 1956.



(a) Helicopter position at emission time
 $H_0 = 439.6 \text{ m}$
 TPP: Tip Path Plane



(b) Blade Tip Geometry



(c)

Figure 1 (Example 1) - Emission Distance, Blade Tip Geometry and Comparison Between Theory and Experiment for a Helicopter in Flight.

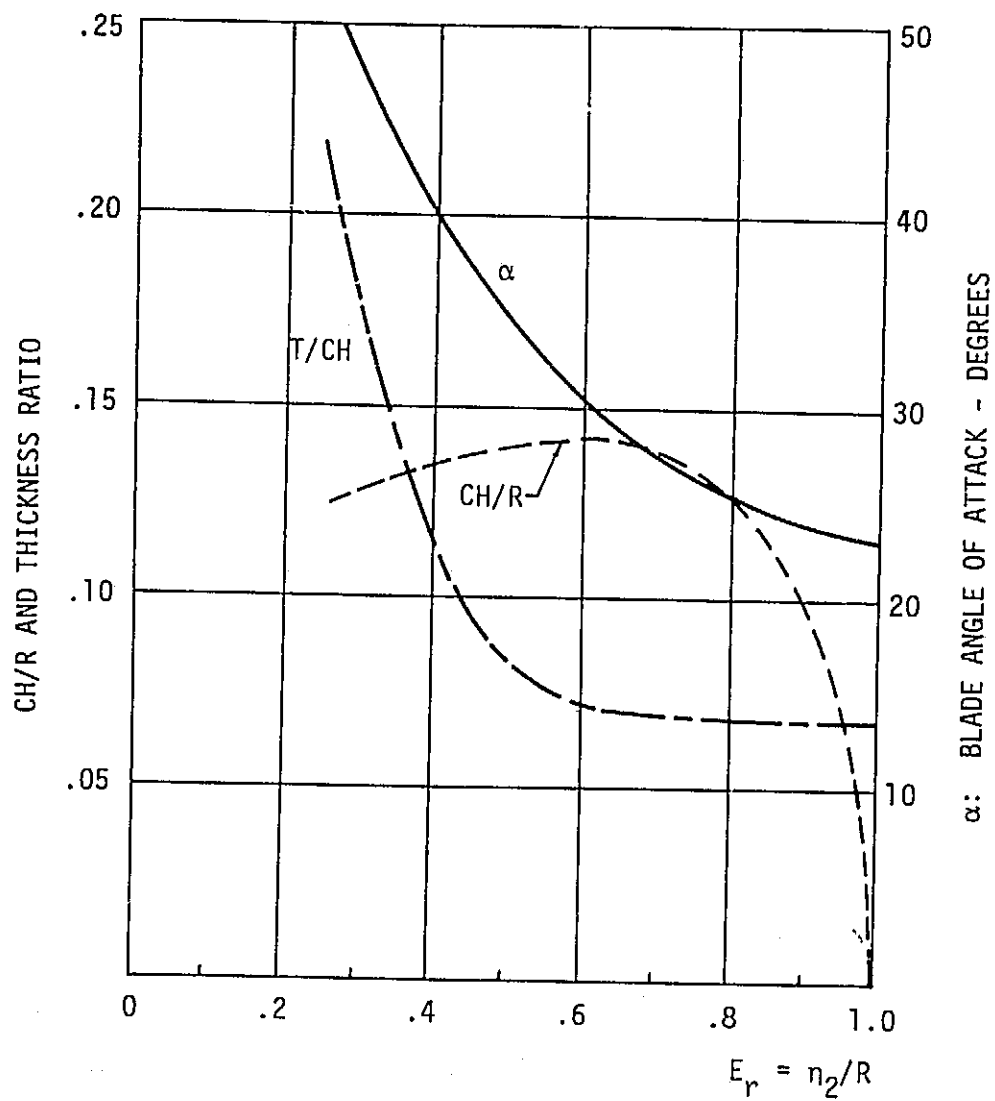


Figure 2 (Example 2) - The Blade Form Curves

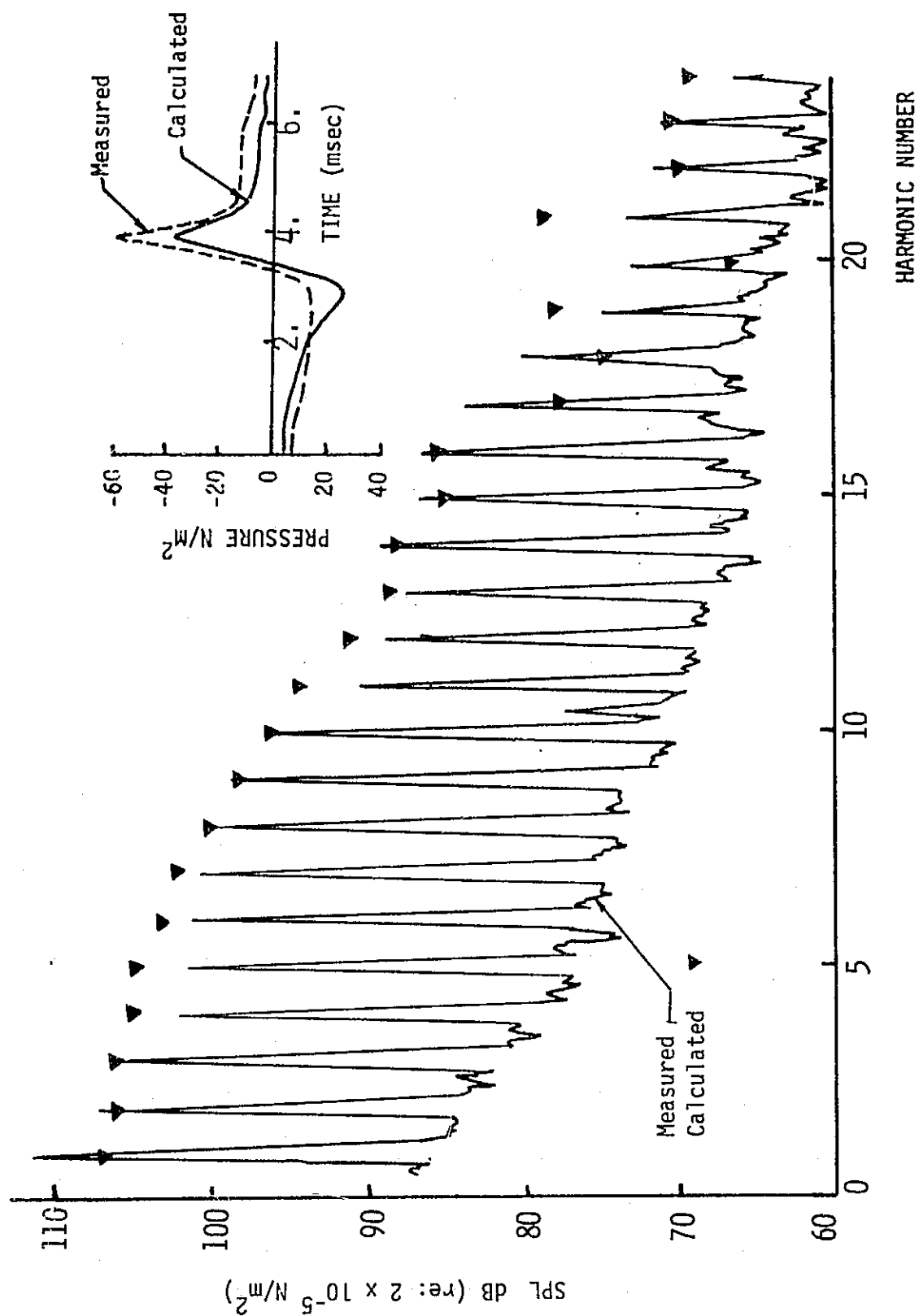
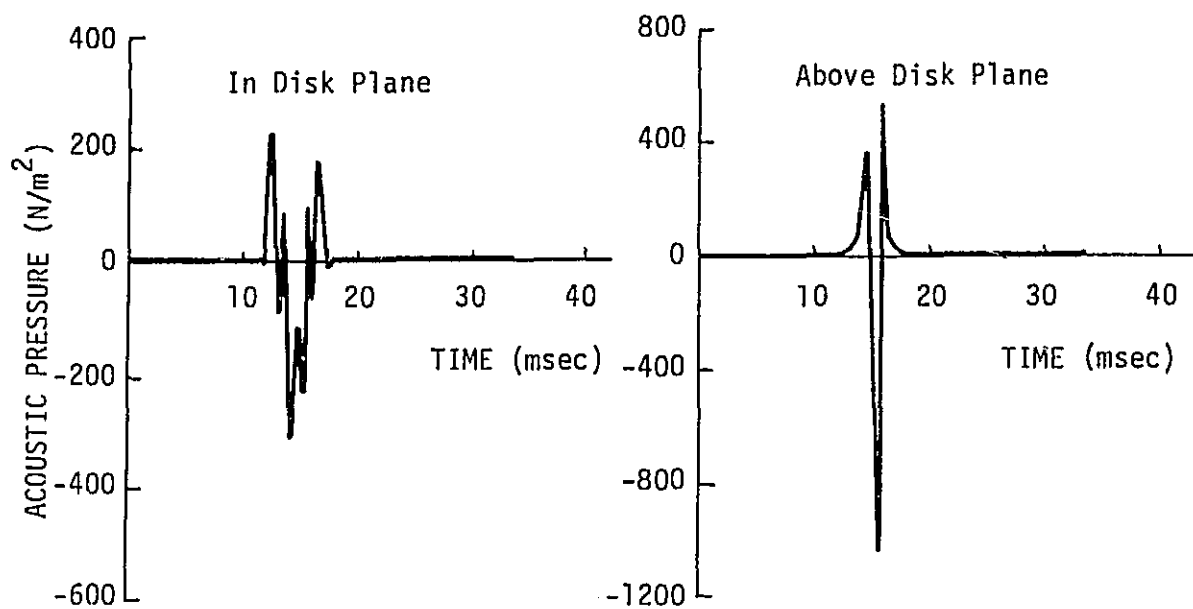


Figure 3 (Example 2) - Comparison of Theory and Experiment for a Propeller in Forward Flight (78 kts). Acoustic Pressure Spectrum and Signature.



Note Change of Pressure Scale

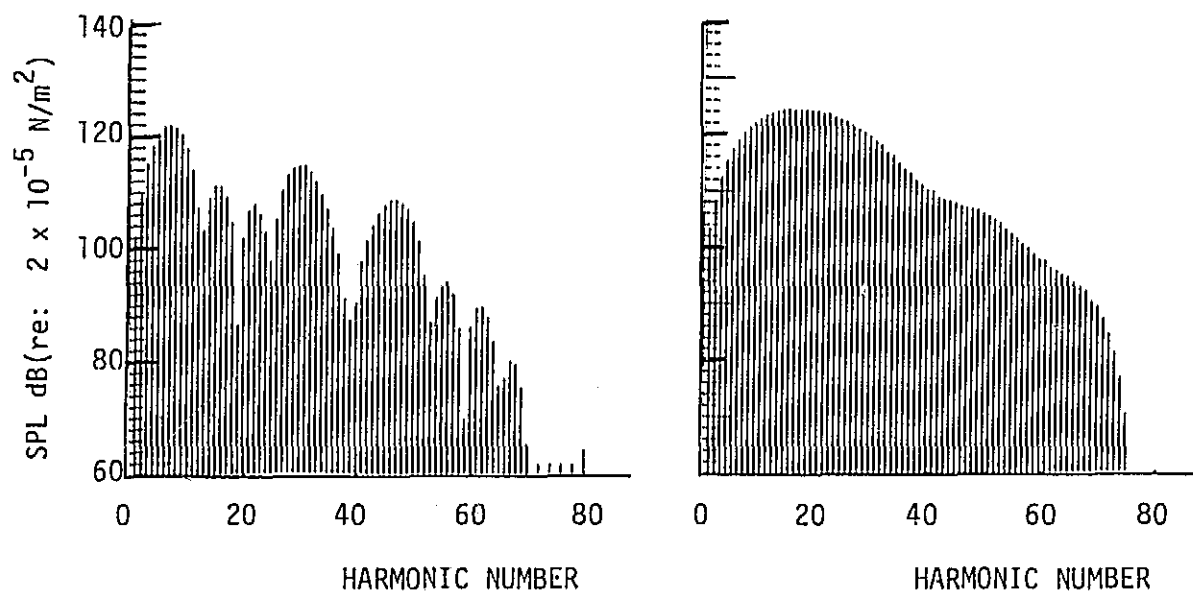
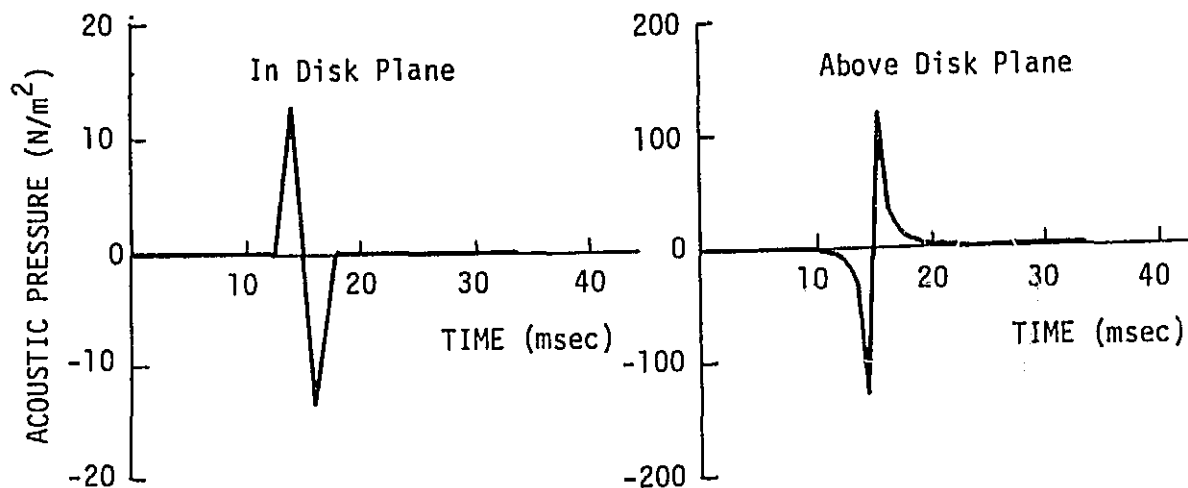


Figure 4 (Example 3) - The Contribution of $\frac{\partial I_1}{\partial t}$ (Thickness Noise), to the Noise of Supersonic Rotating Blades. The Pressure Scale Varies for Each Component of the Noise in This Figure.



Note Change of Pressure Scale

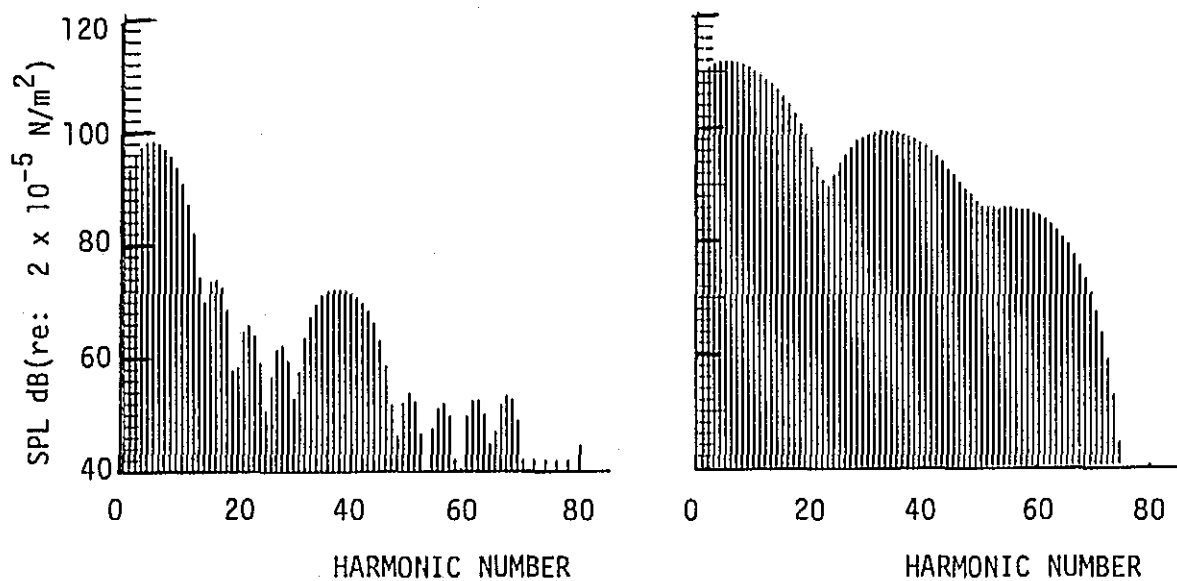


Figure 4 (Cont'd.) - Contribution of $\frac{\partial I_2}{\partial t}$ (Far-Field Loading Noise), Equation 2, to the Noise of Supersonic Rotating Blades.

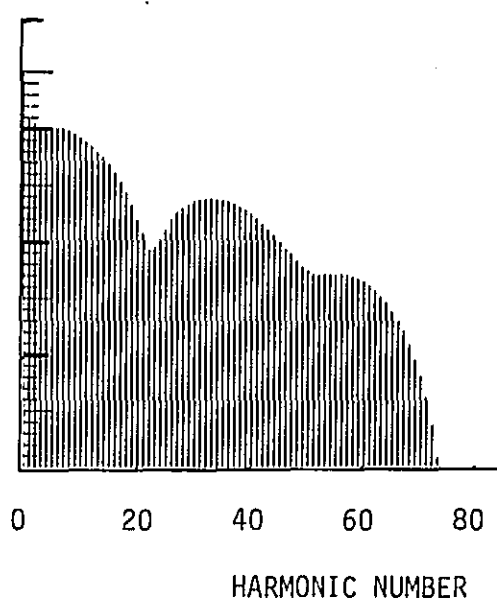
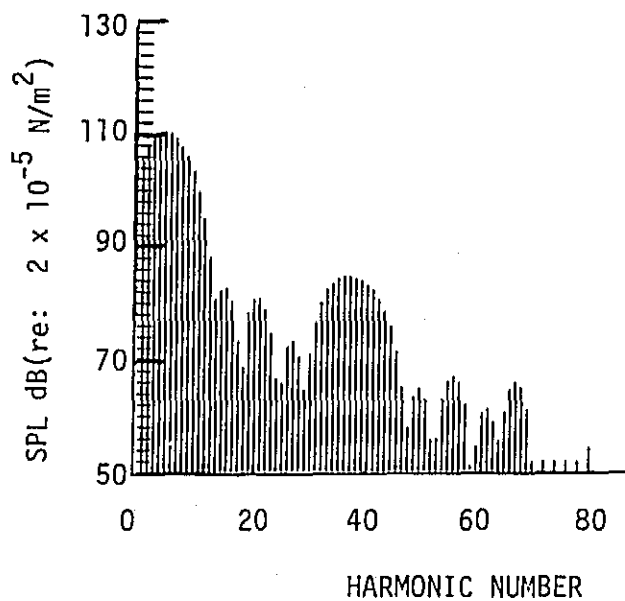
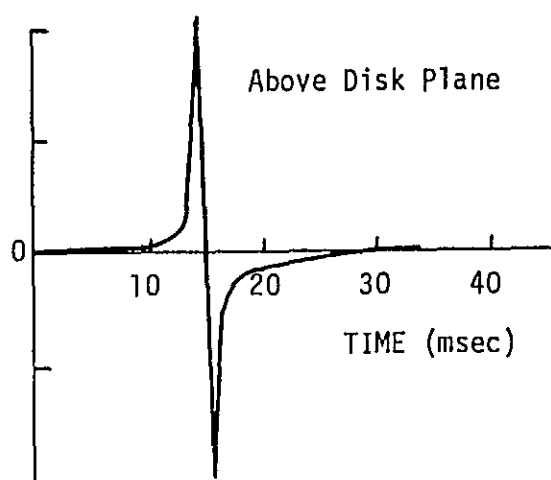
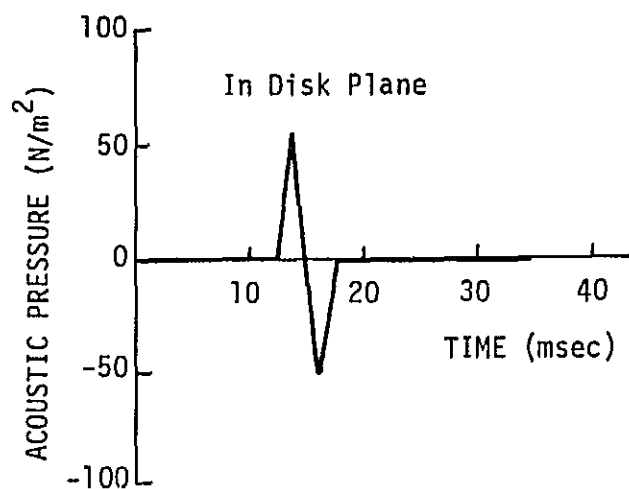
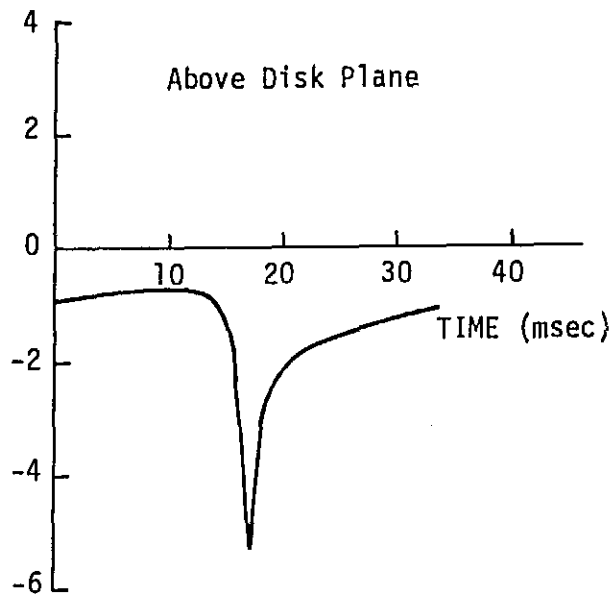
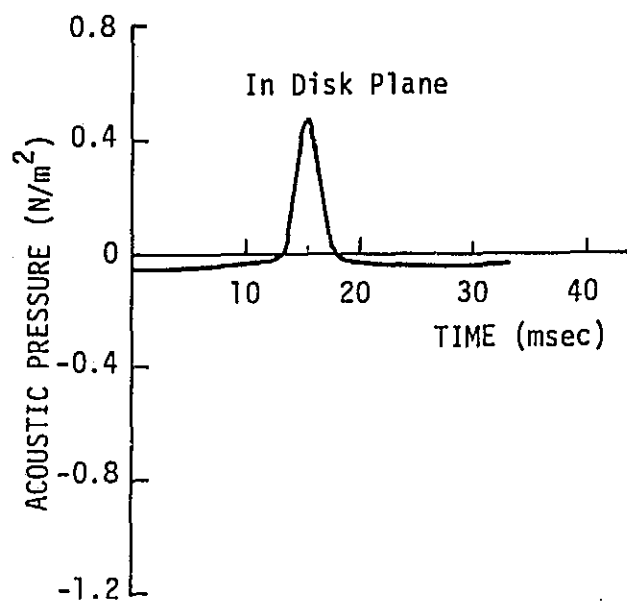


Figure 4 (Cont'd.) - Contribution of $\frac{\partial I_3}{\partial t}$, Equation (2), to the Noise of Supersonic Rotating Blades.



Note Change of Pressure Scale

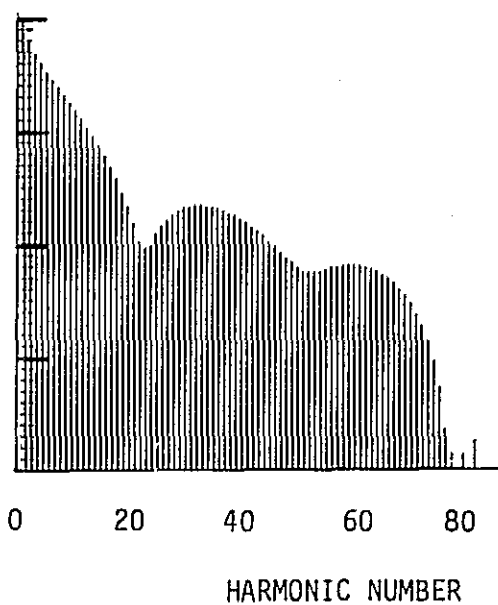
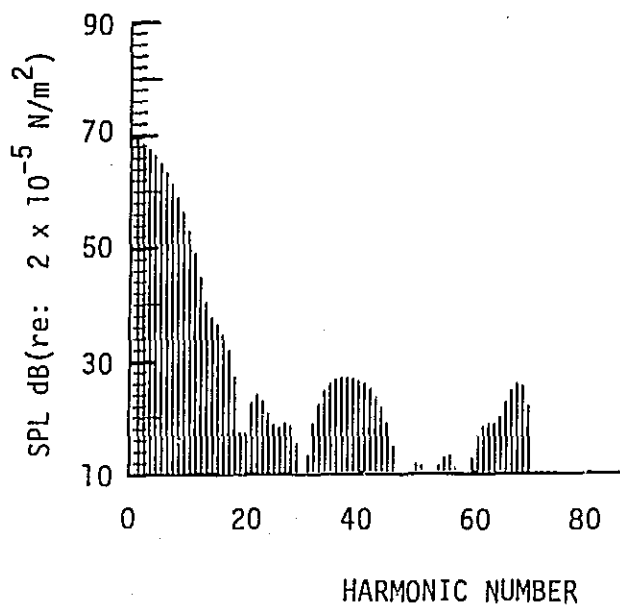


Figure 4 (Cont'd.) - Contribution of I_4 , Equation (2) to the Noise of Supersonic Rotating Blades.

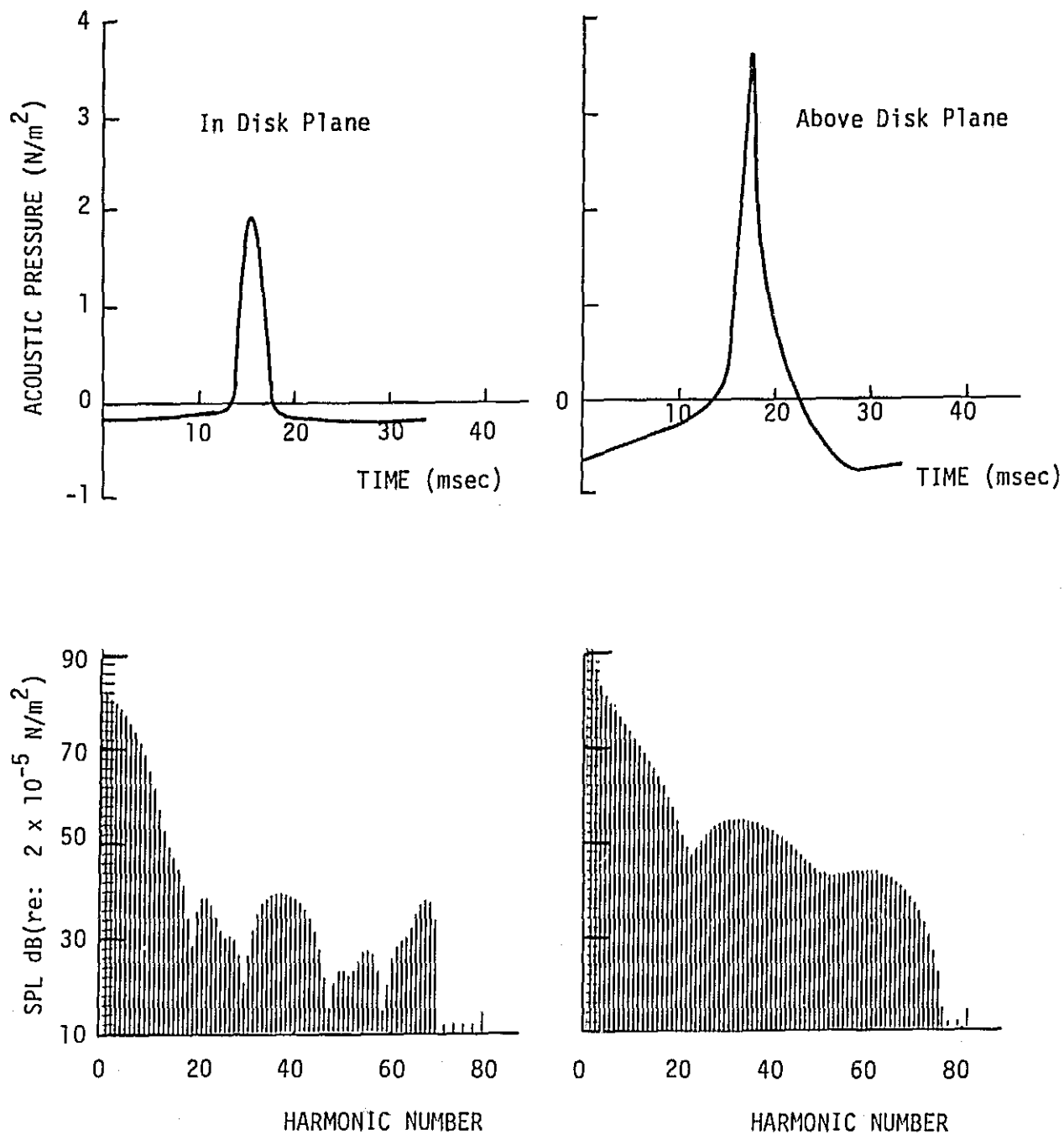
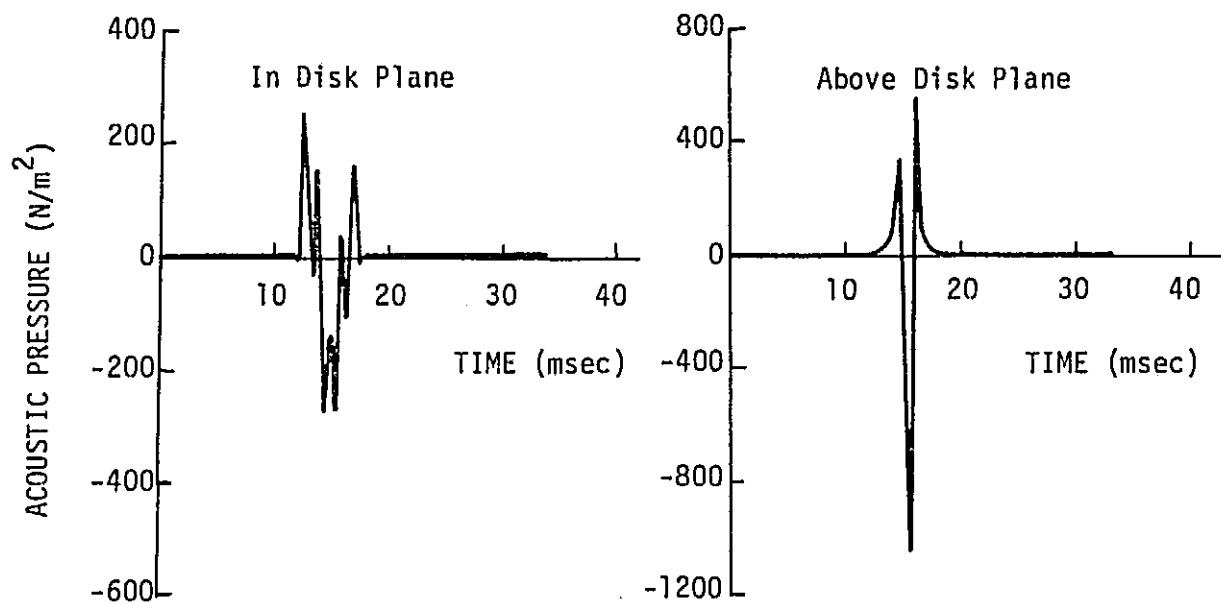


Figure 4 (Cont'd.) - Contribution of I_5 , Equation 2, to the Noise of Supersonic Rotating Blades.



Note Change of Pressure Scale

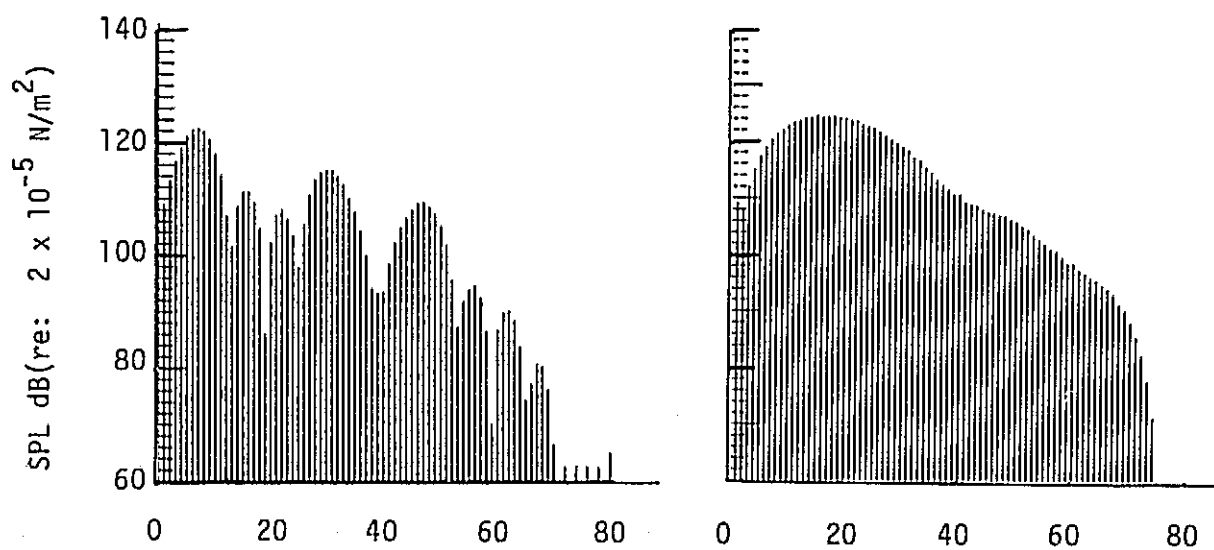


Figure 4 (Concluded) - Overall Acoustic Pressure Signature and Spectrum.

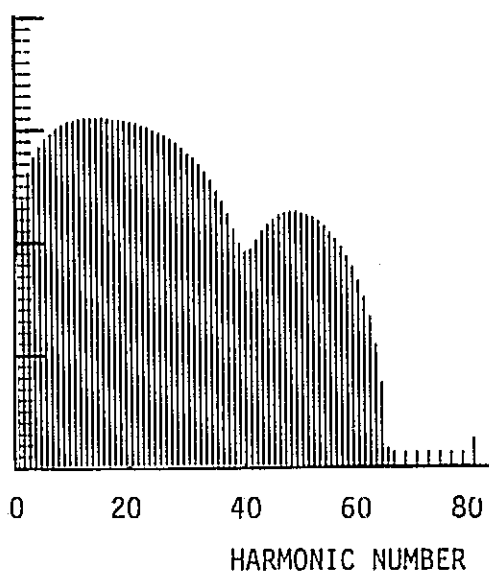
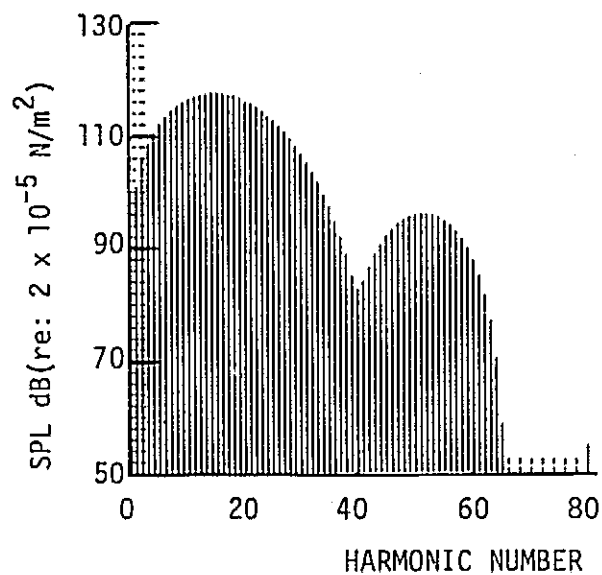
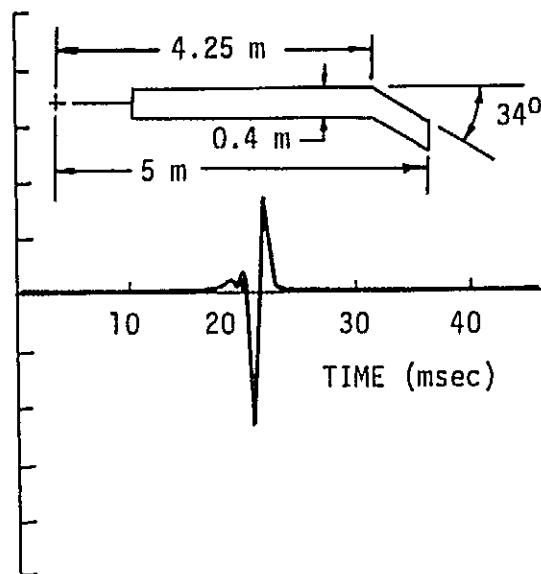
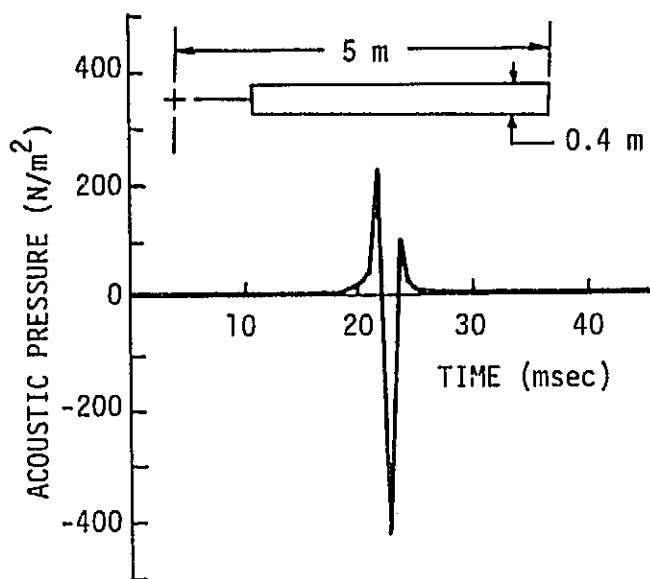


Figure 5 (Example 4) - The Influence of Blade Planform on the Acoustic Pressure Signature and Spectrum of Helicopter Rotor in Flight (Thickness Noise Only).

1. Report No. NASA TM X-74037		2. Government Accession No.		3. Recipient's Catalog No.	
4. Title and Subtitle A New Capability for Predicting Helicopter Rotor and Propeller Noise Including the Effect of Forward Motion				5. Report Date June 1977	
				6. Performing Organization Code 2620	
7. Author(s) F. Farassat and T. J. Brown				8. Performing Organization Report No. NASA TM X-74037	
9. Performing Organization Name and Address NASA Langley Research Center Hampton, Virginia 23665				10. Work Unit No. 505-10-26-02	
				11. Contract or Grant No.	
12. Sponsoring Agency Name and Address National Aeronautics and Space Administration Washington, DC 20546				13. Type of Report and Period Covered Technical Memorandum	
				14. Sponsoring Agency Code	
15. Supplementary Notes Paper presented at the Army Science Conference 1976, West Point, NY					
16. Abstract This paper discusses the governing equation and computing technique for the prediction of helicopter rotor and propeller noise. The method which gives both the acoustic pressure time history and spectrum of the noise includes the thickness and the loading noise. It has been effectively adapted to computers resulting in a new capability in noise prediction by removing many of the restrictions and limitations of previous theories. The capability results from the fact that the theory is developed entirely in the time domain in contrast to most previous works which were developed in frequency domain. The formulation and the technique used is not limited to compact sources, steady level flight or to the far-field. In addition, the inputs to the computer program are normally available or are amenable to experimental measurements. This program can be used to study rotor and propeller noise with the aim of minimizing the radiated noise to reduce annoyance to the public. Several examples demonstrating the features and capability of the computer program are presented.					
17. Key Words (Suggested by Author(s)) (STAR category underlined) Rotor Noise Propeller Noise <u>02, 71</u> Acoustics				18. Distribution Statement Unclassified Unlimited	
19. Security Classif. (of this report) Unclassified		20. Security Classif. (of this page) Unclassified		21. No. of Pages 22	
				22. Price* \$3.50	